Supporting Information: Tailoring the structures and transformations between copper complexes in gas-solid reaction and solid-state synthesis

Haitao Li, Ruhui Li, Fang Guo *

College of Chemistry, Liaoning University, Shenyang 110036, China.

Contents

Table S1. Crystal data and structural refinement parameters for 1–5.

	1	2	3	4	5
Empirical formula	$C_{36}H_{54}Cl_{12}Cu_3N_8$	$C_{18}H_{28}Cl_6CuN_4$	$C_{18}H_{30}Cl_8Cu_2N_4O$	$C_{18}H_{30}Cl_6CuN_4O$	$C_{24}H_{38}Cl_4Cu_2N_6$
Formula weight	1214.92	576.69	729.16	594.71	679.48
Crystal temperature (K)	296	296	173	298	293
Crystal system	Monoclinic	Orthorhombic	Orthorhombic	Monoclinic	Orthorhombic
Space group	*C*2	$P2_12_12$	$P2_12_12_1$	$P2_1$	*I*222
Z	2	4	4	2	4
a(Å)	37.062(3)	12.4243(2)	9.6563(5)	6.9780(6)	10.6438(4)
b(Å)	7.5624(6)	25.8202(5)	11.4146(7)	14.7620(13)	16.6101(7)
c(Å)	9.3156(7)	7.3301(2)	24.6751(14)	12.3395(10)	24.9031(9)
α(deg)	90.00	90.00	90.00	90.00	90.00
β(deg)	96.854(4)	90.00	90.00	100.140(3)	90.00
γ(deg)	90.00	90.00	90.00	90.00	90.00
V(Å^3)	2592.3(4)	2351.48(9)	2719.8(3)	1251.23(18)	4402.7(3)
D_x(Mg.cm^{-3})	1.556	1.629	1.781	1.579	1.025
μ(mm^{-1})	1.873	1.625	2.371	1.532	0.853
F(000)	1234	1180	1472	610	1400
R_{int}	0.0420	0.0275	0.0204	0.0277	0.1532
No.of collected data(unique)	19136	19326	47659	18666	17256
No.of data with I>2σ(I)	5281	5240	6548	5750	4631
No.of parameters varied	344	270	301	272	169
s	1.111	1.071	1.236	1.066	0.996
R_1	0.0788	0.0237	0.0214	0.0303	0.0839
wR_2	0.2314	0.0521	0.0550	0.0749	0.2323

Table S2. Hydrogen bonds in crystal **1**.

	D-H(Å)	D···A(Å)	H···A(Å)	D-H···A(°)	Symmetry Code
N2-H2B···Cl2(i)	0.890(1)	3.256(8)	2.444(4)	151.12(3)	-x+3/2, y-1/2, -z+1
N2-H3B···Cl2(ii)	0.890(4)	3.121(2)	2.667(0)	121.19(8)	-x+3/2, y+1/2, -z+1
N3-H3A···Cl3(iii)	0.889(7)	3.350(6)	2.487(0)	165.59(6)	-x+3/2, y-1/2, -z+1
N2-H2A···Cl4(iv)	0.889(9)	3.173(8)	2.295(2)	169.26(5)	-x+3/2, y-1/2, -z+1
N2-H2B···Cl1(v)	0.890(1)	3.239(2)	2.670(2)	122.72(8)	-x+3/2, y-1/2, -z+1
N3-H3A···Cl1(vi)	0.890(4)	3.099(7)	2.304(1)	148.71(3)	-x+3/2, y-1/2, -z+1
N4-H4···Cl6(vii)	0.860(5)	3.353(1)	2.626(7)	142.85(1)	x, y-1, z

Table S3. Hydrogen bonds in crystal **2**.

	D-H(Å)	D···A(Å)	H···A(Å)	D-H···A(°)	Symmetry Code
N2-H2B···Cl1(i)	0.899(2)	3.085(4)	2.000(0)	173.72(3)	x, y, z
N3-H3B···Cl1(ii)	0.890(3)	3.084(8)	2.201(0)	171.80(1)	x, y, z
N2-H2A···Cl2(iii)	0.890(0)	3.055(9)	2.184(7)	165.69(4)	x, y, z
N1-H1···Cl1(iv)	0.929(7)	3.248(0)	2.557(1)	131.43(4)	-x+1, -y+1, z
N1-H1···Cl2(v)	0.930(0)	3.289(6)	2.577(7)	133.72(1)	-x+1, -y+1, z-1
N4-H4···Cl4(vi)	0.852(7)	3.164(5)	2.407(6)	148.20(6)	-x+1/2, y-1/2, -z+1
N4-H4···Cl5(vii)	0.852(7)	3.411(0)	2.801(4)	129.87(8)	-x+1/2, y-1/2, -z+1

Table S4. Selected bond lengths (Å) and angles (º) for **5**.

N1-Cu1	2.0140(56)	Cu1-Cl1	2.5536(12)
N2-Cu1	2.1088(55)	Cu1-Cl2	2.2992(17)
N3-Cu1	1.9614(54)	C7-C12	1.5648(90)
C7-N2	1.4934(92)	C12-N3	1.4672(92)
N1-Cu1-Cl2	89.518(16)	N1-Cu1-Cl1	97.395(18)
N2-Cu1-N3	83.279(21)	N2-Cu1- Cl1	92.136(17)
N2-Cu1- Cl2	162.783(15)	N1-Cu1-N2	92.411(214)
Cl2-Cu1- Cl1	104.585(53)		
Cu1-Cl1-Cu1	116.773(26)		

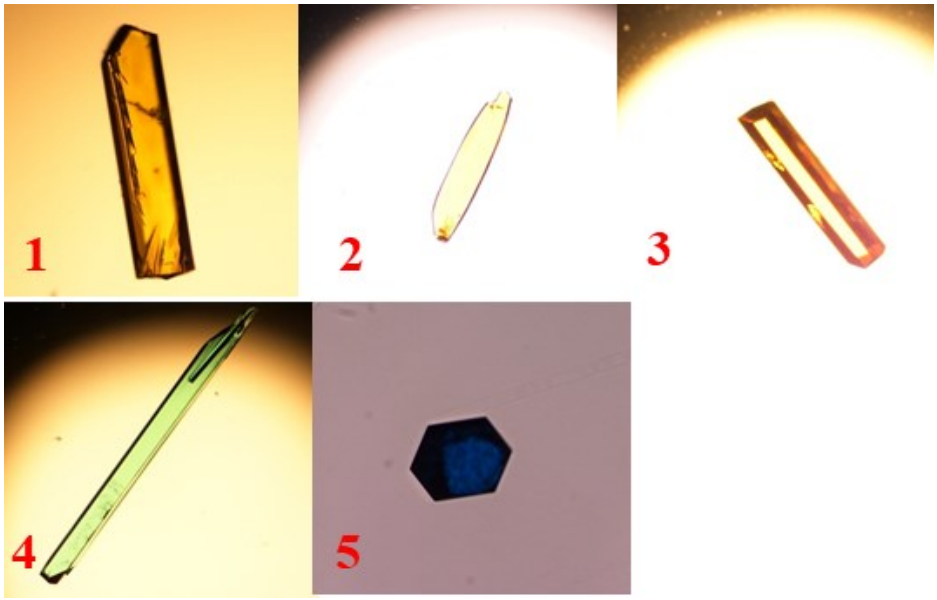

Figure S1. Images of the crystals.

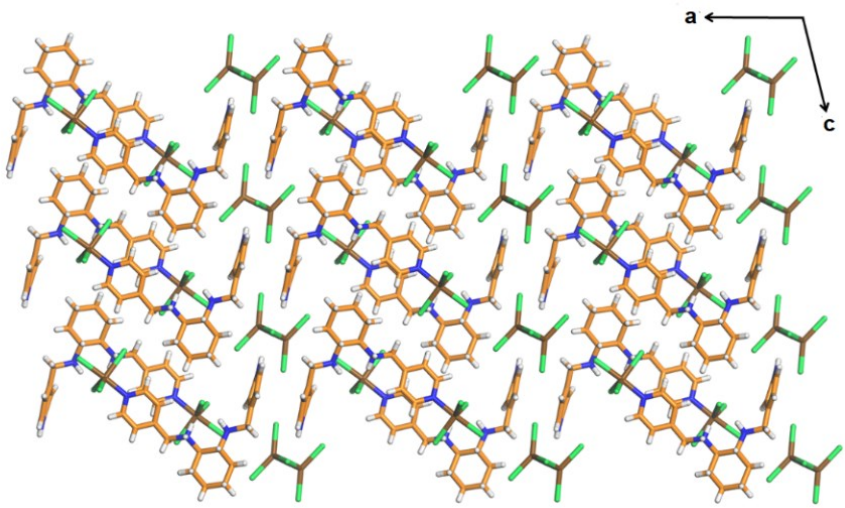

Figure S2. Packing of **1** viewed along the *b*-axis.

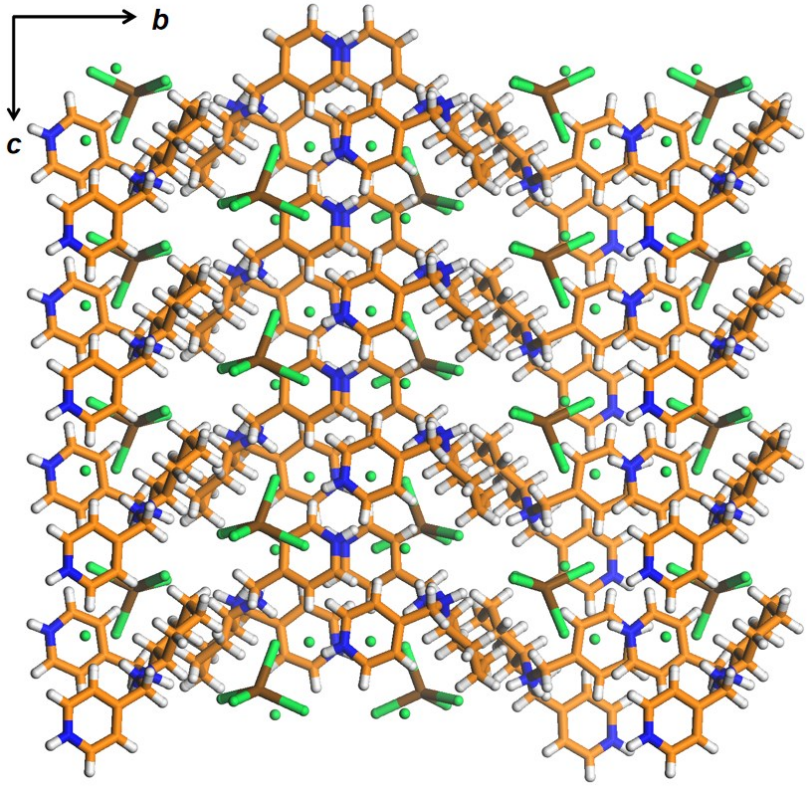

Figure S3. Packing of **2** viewed along the *a*-axis.

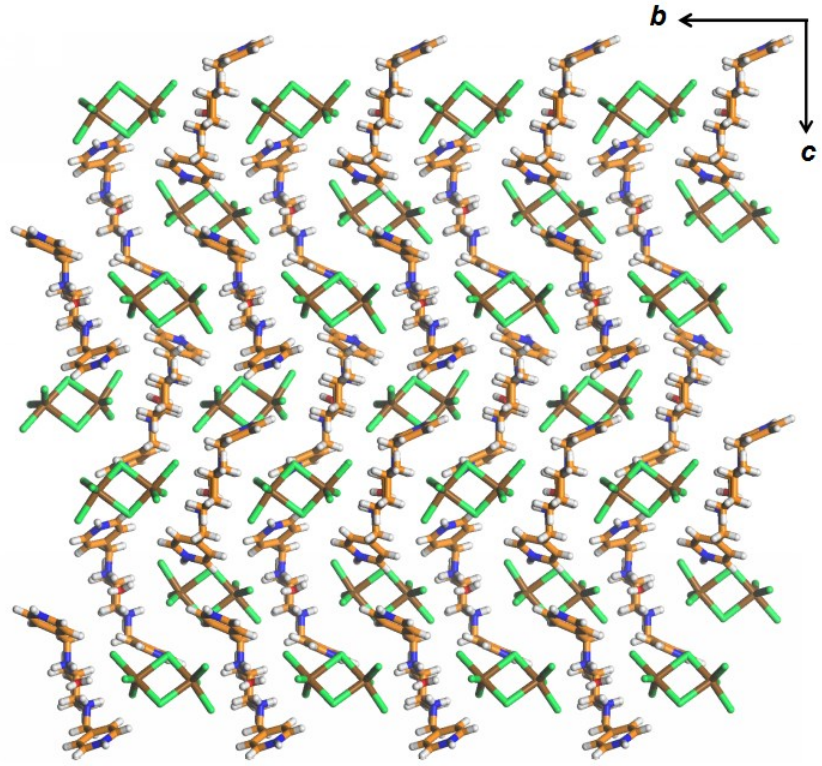

Figure S4. Packing of **3** viewed along the *a*-axis.

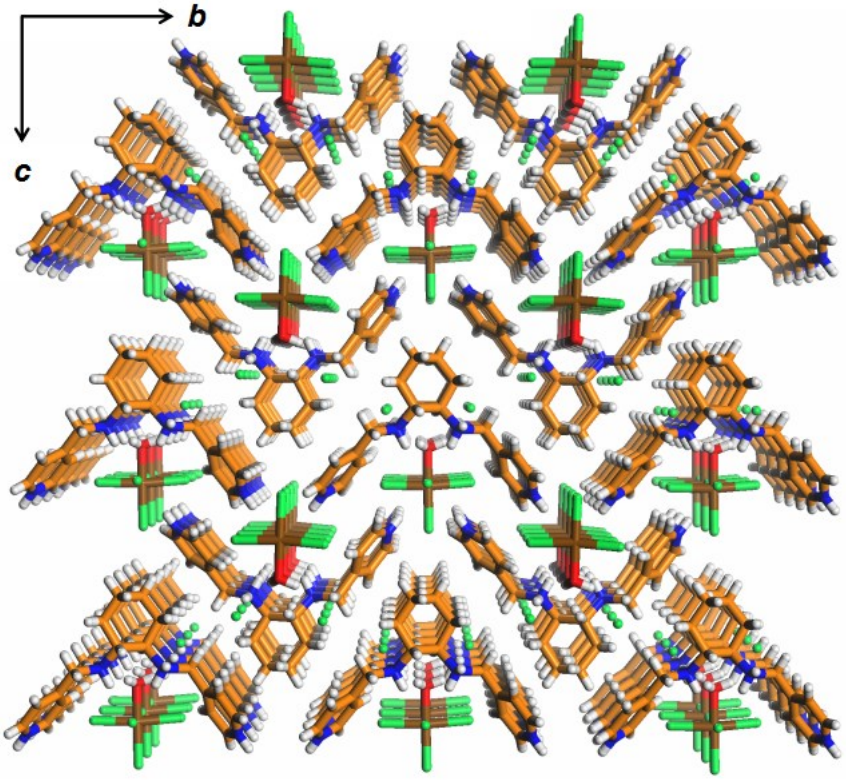

Figure S5. Packing of **4** viewed along the *a*-axis.

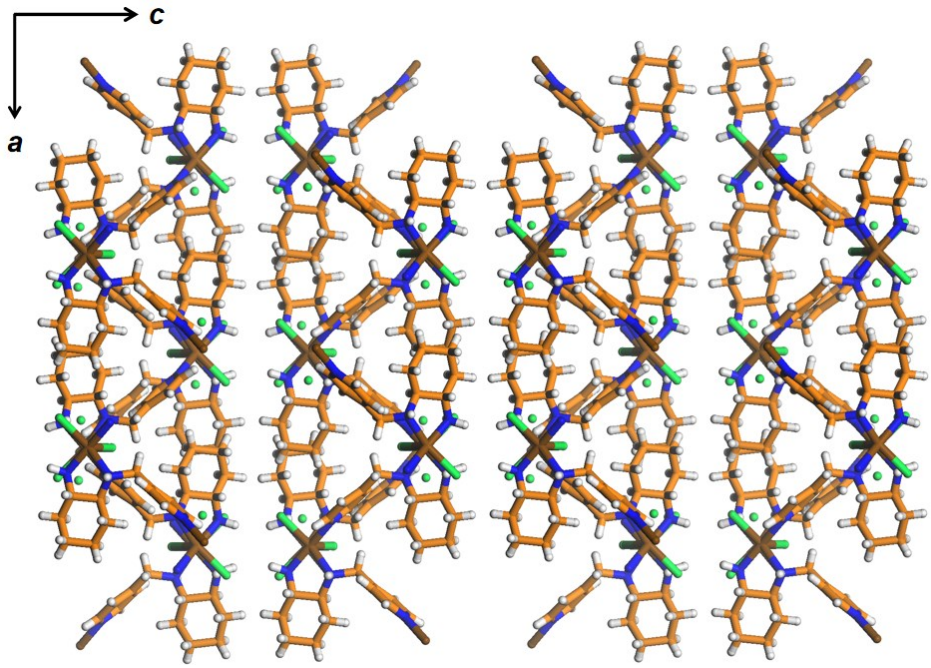

Figure S6. Packing of **5** viewed along the *b*-axis.

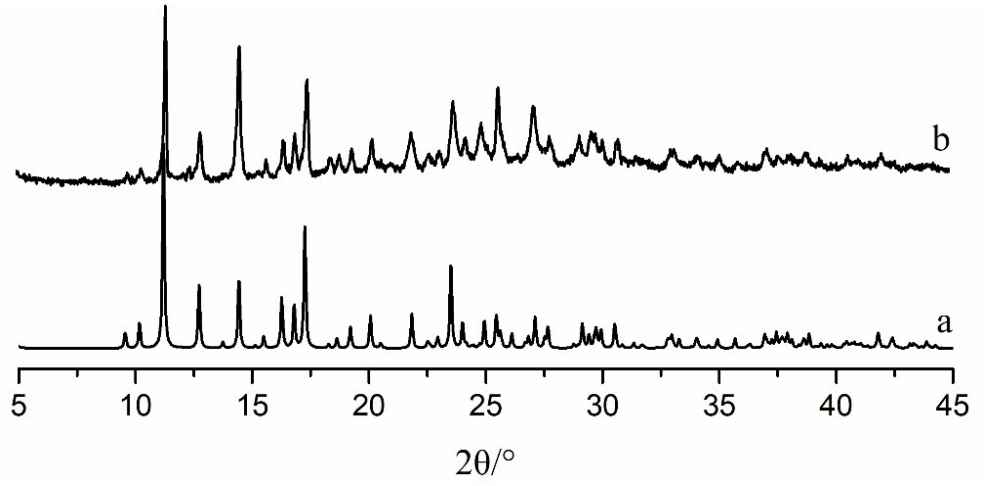

Figure S7. Comparison PXRD patterns of crystal **1**: (a) Simulated PXRD from single crystal **1**; (b) Experimental PXRD from single crystal **1**.

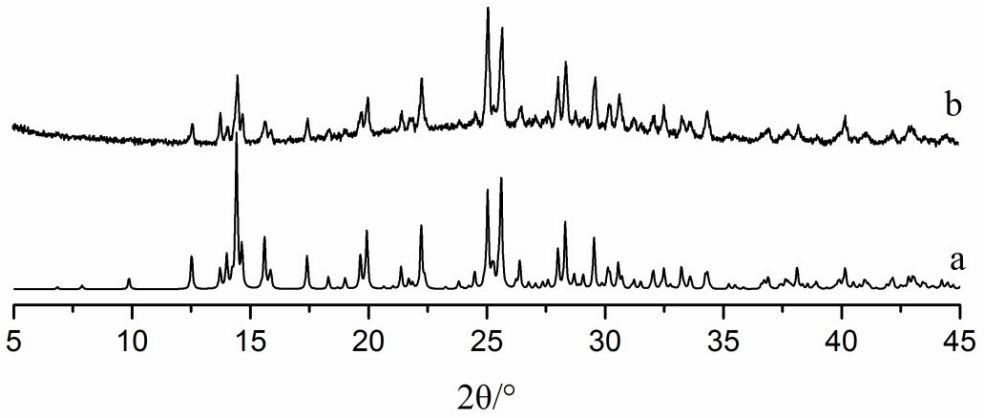

Figure S8. Comparison PXRD patterns of crystal **2**: (a) Simulated PXRD from single crystal **2**; (b) Experimental PXRD from single crystal **2**.

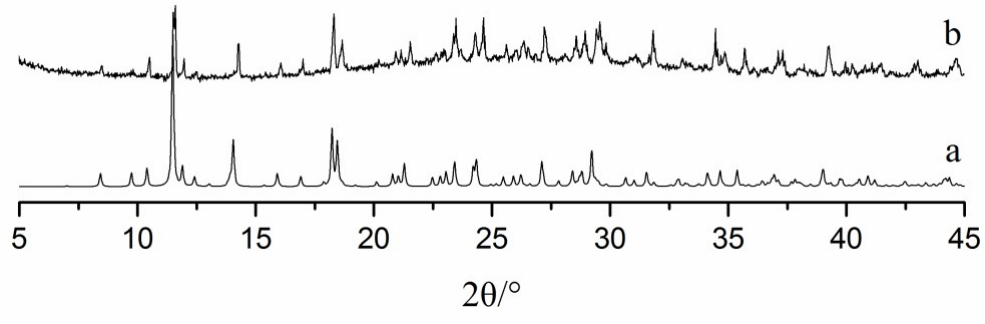

Figure S9. Comparison PXRD patterns of crystal **3**: (a) Simulated PXRD from single crystal **3**; (b) Experimental PXRD from single crystal **3**.

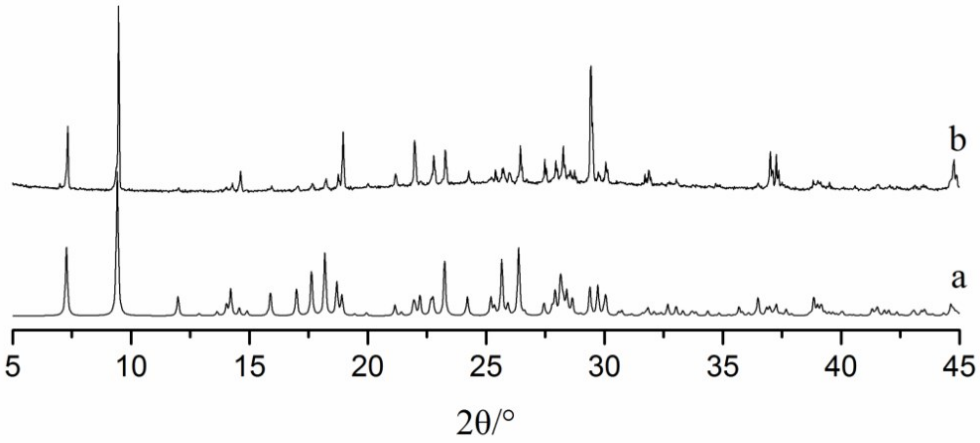

Figure S10. Comparison PXRD patterns of crystal **4**: (a) Simulated PXRD from single crystal **4**; (b) Experimental PXRD from single crystal **4**.

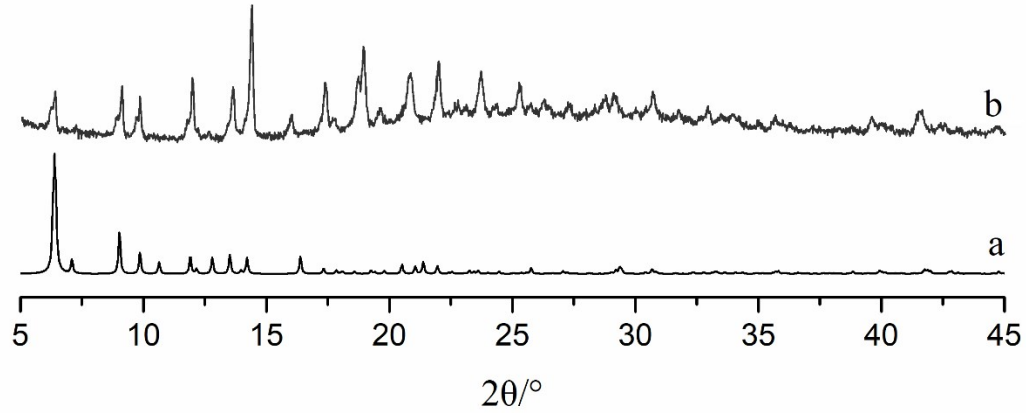

Figure S11. Comparison PXRD patterns of crystal **5**: (a) Simulated PXRD from single crystal **5**; (b) Experimental PXRD from single crystal **5**.

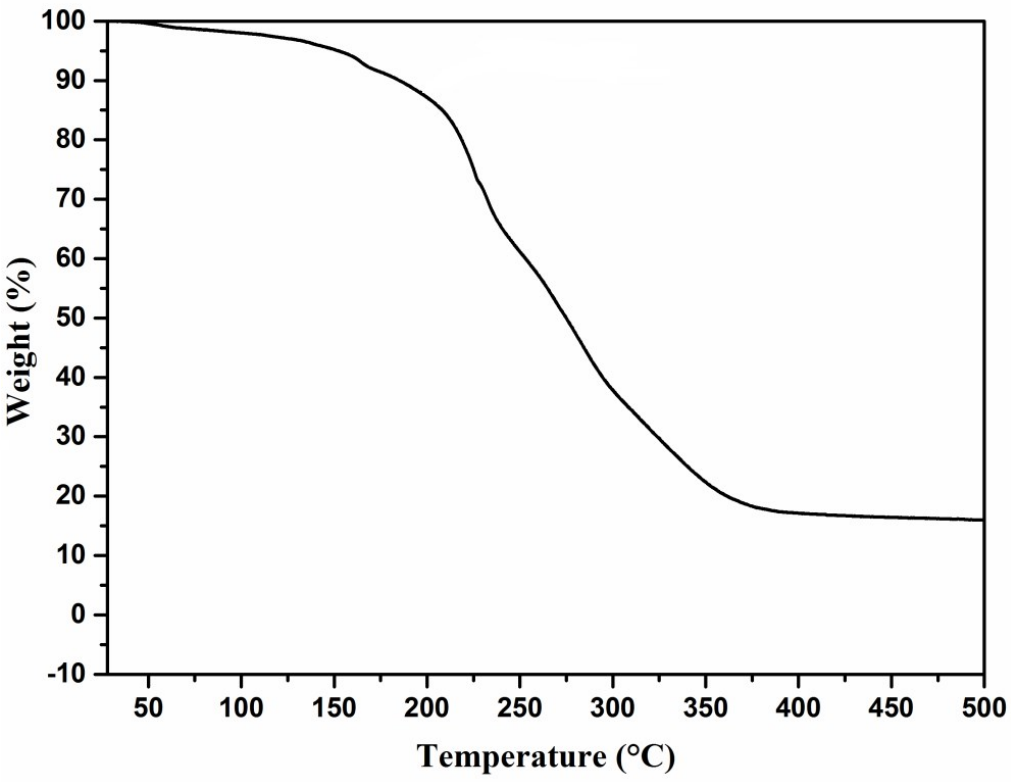

Figure S12. TGA analysis for crystal **1**. Equivalents of HCl molecules were released on heating to 195 °C (obsd. 11.56%, calcd. 12.02%), further heating led to collapse of the crystal structure.

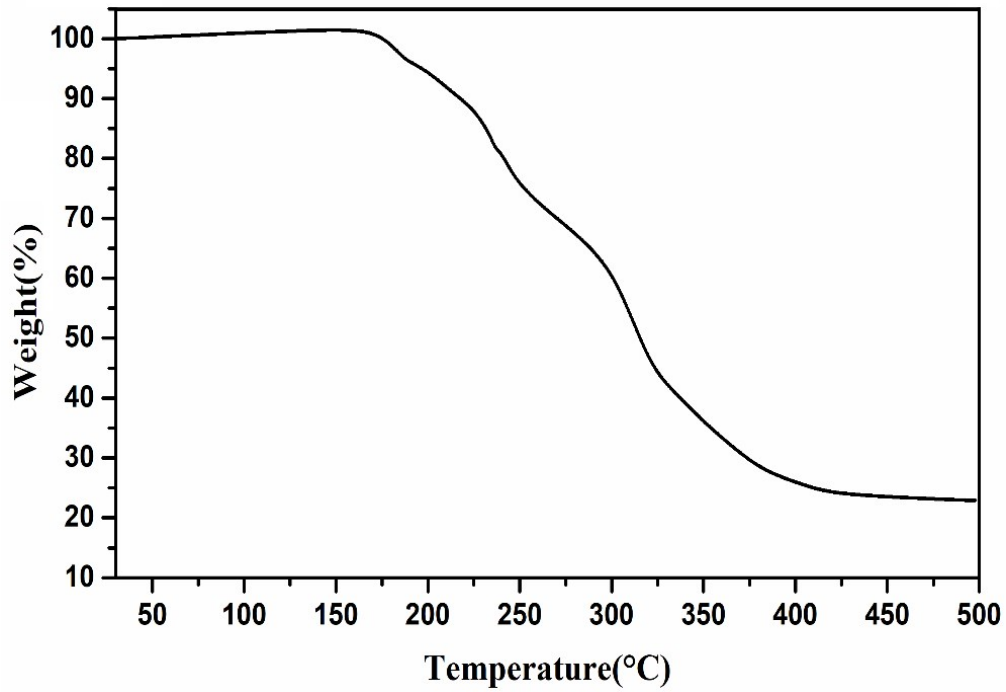

Figure S13. TGA analysis for crystal **2**. The four HCl molecules were released on heating to 255 °C (obsd. 25.70%, calcd. 25.35%), further heating led to collapse of the crystal structure.

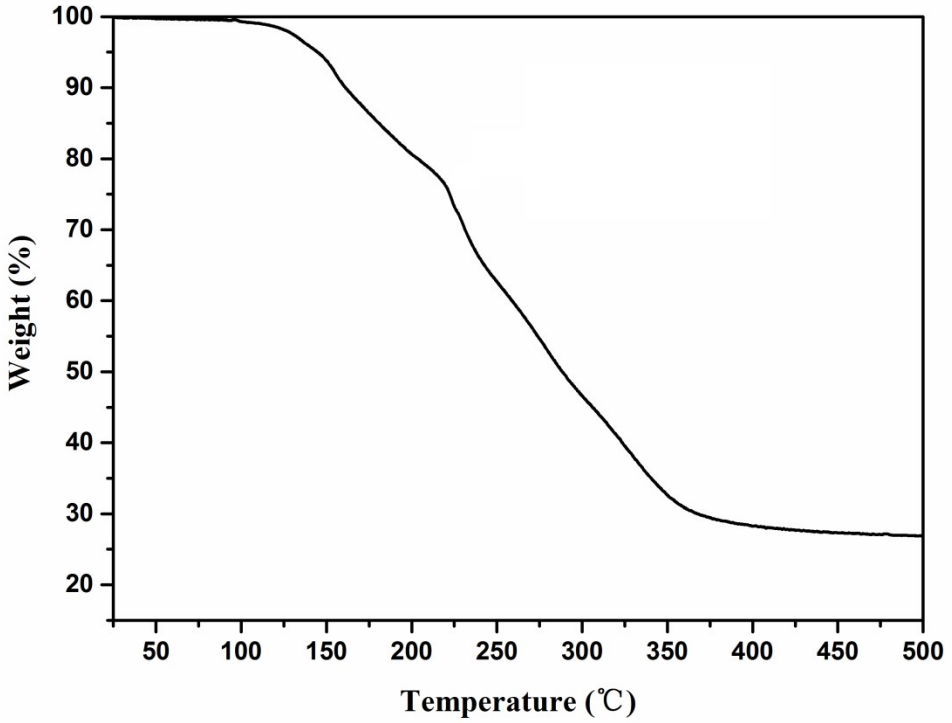

Figure S14. TGA analysis for crystal **3**. The weight loss of the water molecules and four HCl molecules were released on heating to 219 °C (obsd. 24.59%, calcd. 27.61%). Further heating led to the loss of the ligand.

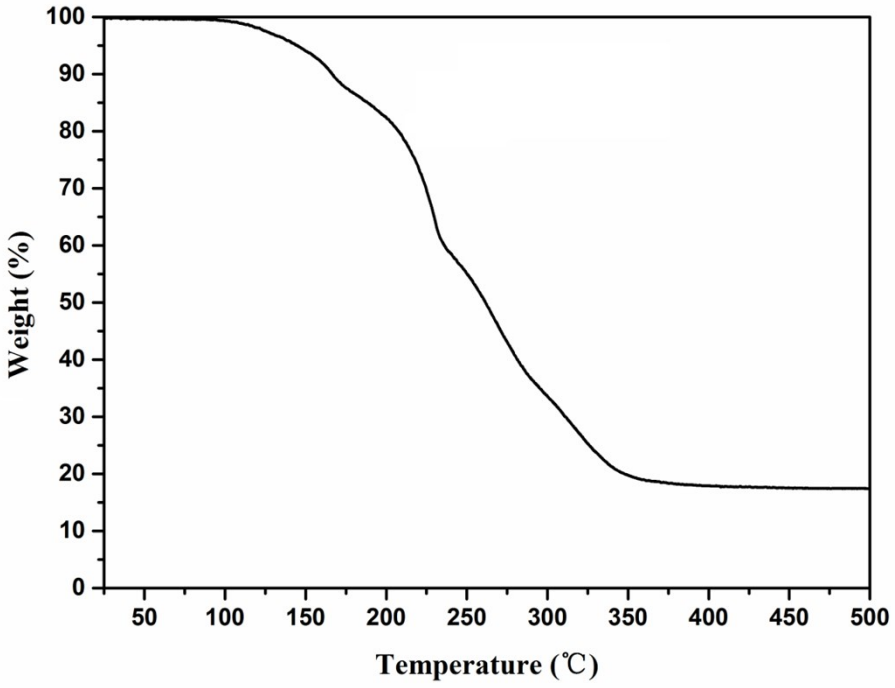

Figure S15. TGA analysis for crystal **4**. Water molecules and four HCl molecules were released on heating to 221 °C (obsd. 26.70%, calcd. 28.25%). Further heating led to the loss of the ligand.

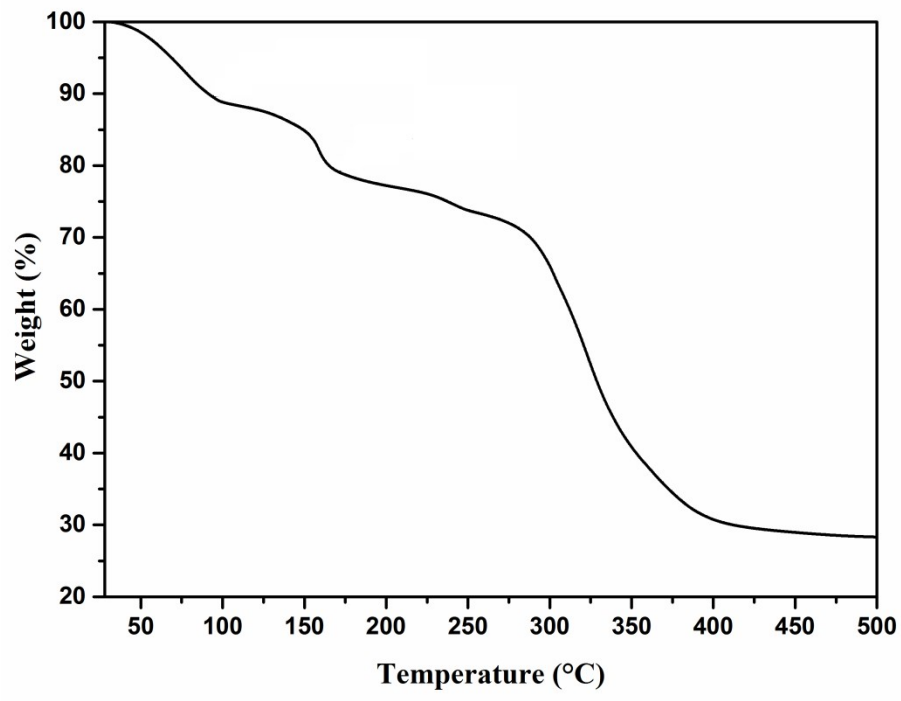

Figure S16. TGA analysis for crystal **5**. The water molecules (*i.e.*, the H_2O in channel) were released from r.t. to 98 °C (obsd. 11.35%, calcd. 11.70%), the guest molecules (Cl^-) were released on heating from 123 to 171 °C (obsd. 10.45%, calcd. 10.61%), further heating led to collapse of the crystal structure.

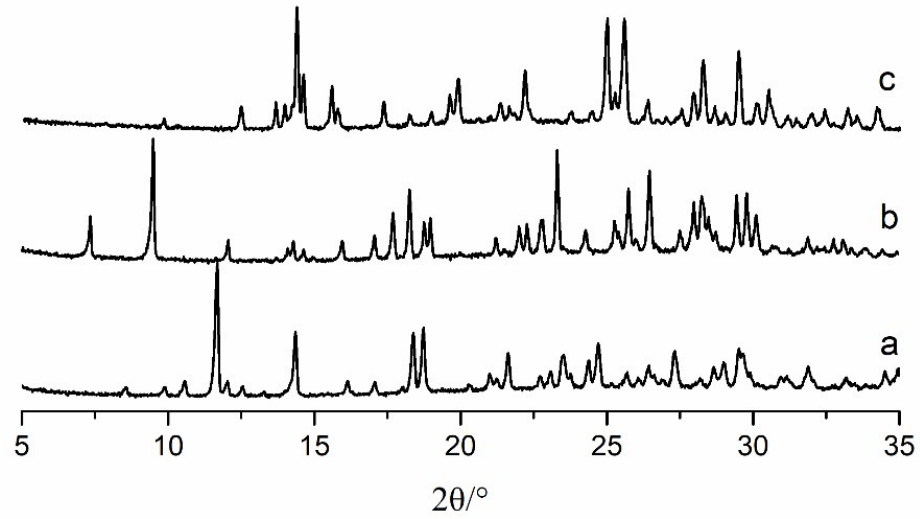

Figure S17. Comparison of PXRD patterns of grinding salt **3** with equimolar protonated L: (a) measured for crystal **3**. (b) measured for the grinding product of **3** and protonated L in ratio of 1:1. (c) measured for crystal **2**.

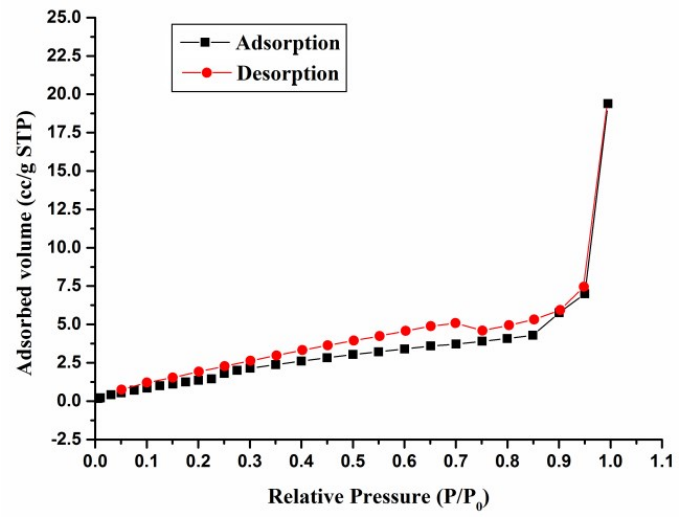

Figure S18. Nitrogen adsorption/desorption isotherms of the powder of **5**.

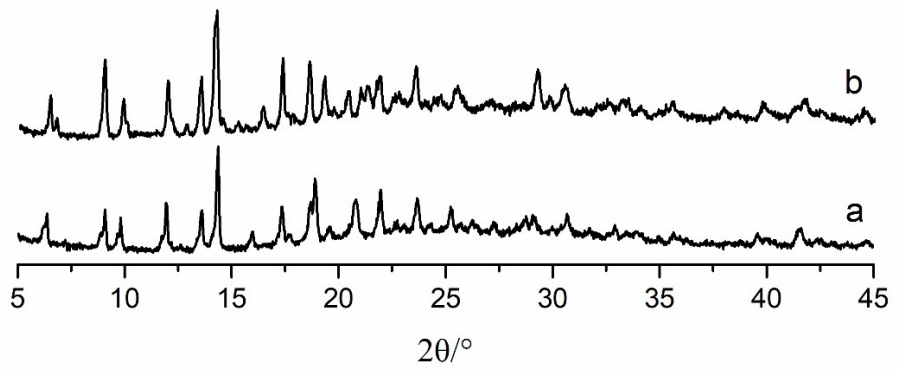

Figure S19. PXRD patterns of coordination polymer **5** at (a) r.t. (b) 98 °C for 1 h.

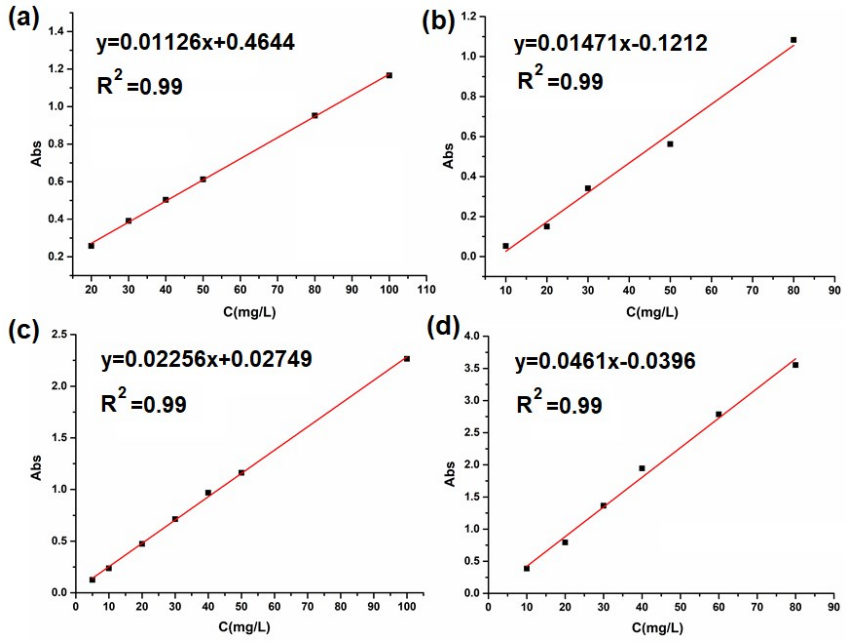

Figure S20. The calibration curve of (a) CR, (b) MB, (c) OG and (d) I_2 in ethanol solutions.

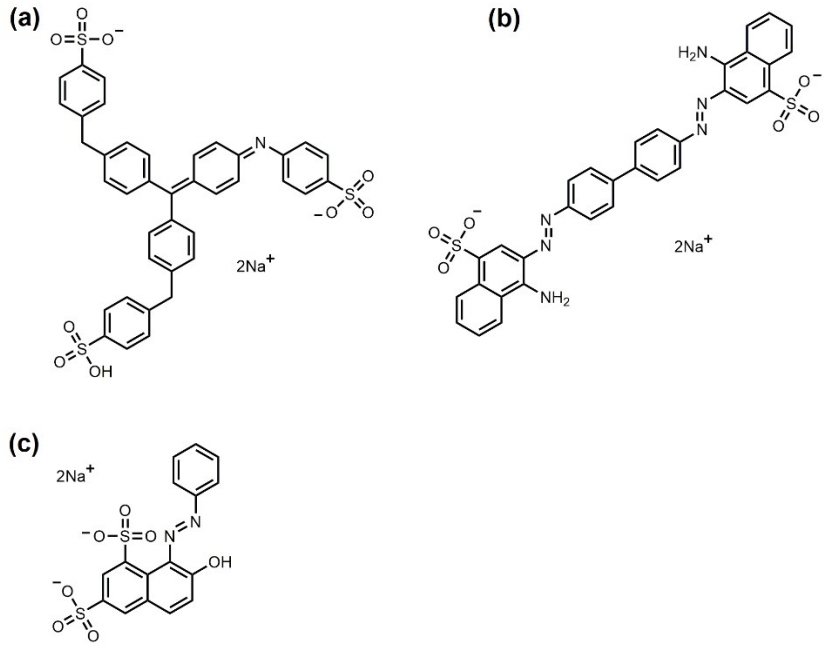

Figure S21. The chemical structure of (a) CR, (b) MB and (c) OG.

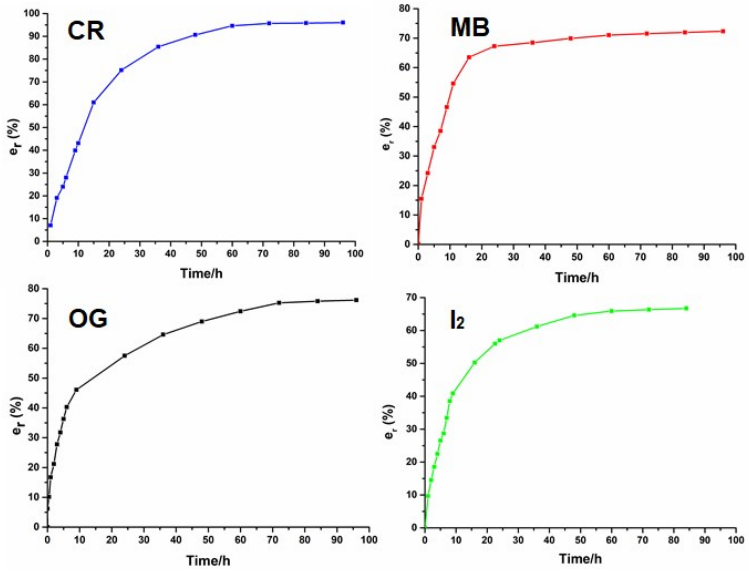

Figure S22. The time-removal efficiency curve of the dyes.

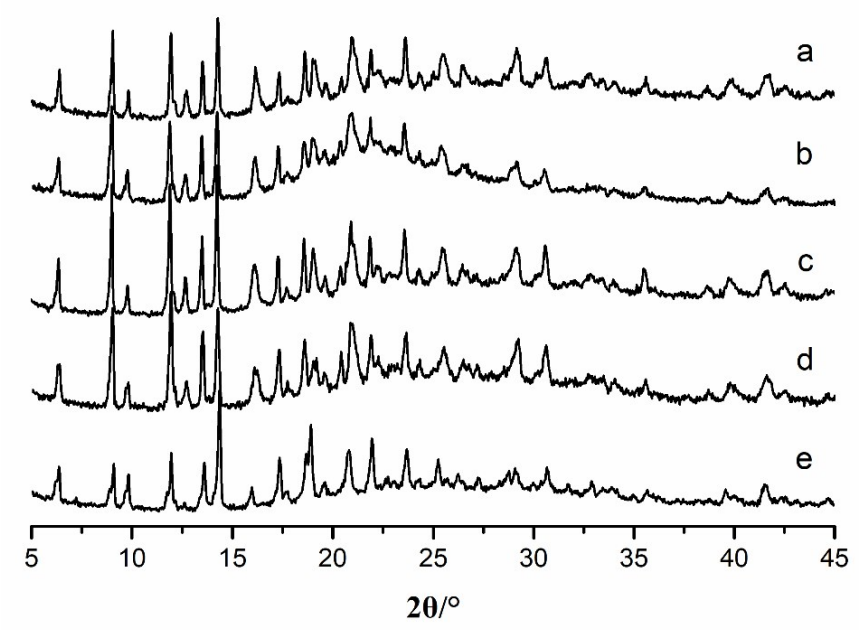

Figure S23. PXRD patterns of (a) CR-loaded **5**, (b) MB-loaded **5**, (c) OG-loaded **5**, (d) I_2-loaded **5** and (e) as-synthesized **5**.